Instantaneous flowrate measurements in high-pressure liquid flows

PAPER • OPEN ACCESS

Instantaneous flowrate measurements in high-pressure liquid flows

To cite this article: A Ferrari *et al* 2023 *J. Phys.: Conf. Ser.* **2648** 012086

View the article online for updates and enhancements.

Instantaneous flowrate measurements in high-pressure liquid flows

A Ferrari[1], P Pizzo[2], M Rundo[1] and O Vento[1,3]

[1] Energy Department, Politecnico di Torino, Corso Duca degli Abruzzi 24, 10129 Torino, Italy
[2] Rabotti Srl, Via Gino Capponi 13, 10148, Torino, Italy

[3] Corresponding author: oscar.vento@polito.it

Abstract. A new flowmeter suitable for high-pressure flows and with a prompt dynamic response is presented. It is constituted by two pressure transducers installed on the monitored high-pressure pipe at a fixed distance one from the other, together with a low-pressure flowmeter that provides a time-averaged flowrate. The measurement algorithm consists of an ordinary differential equation obtained by combining the mass conservation partial differential equation and the momentum balance one applied to the considered piece of pipe comprised between the two pressure transducers. Due to the absence of a master instrument that can be employed as reference to verify the consistency of the measured flowrate, the flowmeter accuracy has been demonstrated by means of numerical models of various hydraulic components, rigorously validated through pressure measurements. The flow ripple of gear pumps has been measured, as well as the flowrate entering a Common Rail injector. For all these cases, the measured flowrate and the one obtained by means of the numerical model are in very good agreement, leading to a robust validation of the presented measurement device.

1. Introduction

A measurement of a high-pressure instantaneous flowrate in fluid power hydraulic circuits can only be obtained by building numerical models that take into consideration all primary hydraulic, mechanical, and electromagnetic features. These models need a thorough validation process against experimental data to ensure appropriate accuracy [1]. This method emphasizes the lack of a flowmeter with the following qualities: small and non-invasive dimensions, great dynamic response, and capacity to operate in a wide pressure range.

For the flowrate measurement, many technologies and working principles have been established. The frequency caused by the impeller rotation, which is directly correlated with the flowrate, is measured in turbine flowmeters [2]. These devices, calibrated in steady state conditions, can be used to monitor unsteady flow rates [3], although only pulsing [4,5], or intermittent [6] flows with frequencies less than 1 kHz can be considered.

Because of their simple construction and installation, orifice flowmeters are widely used in industry [7,8]. Nevertheless, they are primarily utilized for steady-state flows [9], and specific correction curves must be applied to adjust the steady equation for pulsing flows [10].

Electromagnetic flowmeters can be used for flows with a high frequency content, but the requirement for the electrical conductivity of the measured fluid to be less than 0.1 µS/cm precludes the use of this type of flowmeter for diesel or gasoline, as both have a much lower conductivity than the aforementioned threshold [11].

Presently existing Coriolis flowmeters can detect flow rates with pressures up to roughly 400 bar [12], however, actual diesel injection systems can achieve pressure levels of up to 3000 bar [13], while the 500 bar target represents the objective of next generation GDI systems [14]. Besides this, the invasiveness of this class of devices may restrict its applicability [15].

Because of the miniaturization and dynamic response properties of pressure sensors, flowrate estimation based on instantaneous pressure traces provides a particularly appealing prospect in this context [16]. If the hydraulic system is designed so that pressure waves propagate in a single direction, a mathematical relationship between a single pressure time history and the flowrate can be established for each pipe segment [17]. However, if the pressure waves travel back and forth along the pipe, as in a Common Rail system rail-to-injector pipe [18], one pressure signal is insufficient for a consistent flowrate time distribution evaluation.

In this work, a new flowmeter that is capable to measure the instantaneous flowrate in high-pressure liquid flows is presented. It has been employed for the measurement of the delivered flowrate by volumetric pump and of the flowrate entering a Common Rail injector during the injection event. The flowmeter validation has been performed by means of numerical model of the analysed hydraulic layouts.

2. Flowmeter algorithm

The instantaneous high-pressure flowmeter, manufactured by Rabotti and labelled as Flotec, is made up of two pressure transducers, p_{up} and p_{down}, which are mounted at a certain distance, L, in the monitored pipe. The flowmeter algorithm is based on a coupled solution of the partial differential equations for mass conservation and momentum balance formulated for a one-dimensional duct [19]:

$$\begin{cases} \frac{d\rho}{dt} + \rho\frac{\partial u}{\partial x} = 0 \\ \frac{\partial u}{\partial t} + u\frac{\partial u}{\partial x} + \frac{1}{\rho}\frac{\partial p}{\partial x} = -\frac{4\tau_w}{\rho d} \end{cases} \quad (1)$$

where p, ρ and u represent the cross-section averaged flow pressure, flow density and flow velocity, respectively, d is the pipe diameter, t represents the time, x is the spatial coordinate aligned with the duct axis and τ_w represents the wall shear stress. By assuming the incompressible flow hypothesis, the mass conservation and momentum balance equations can be combined as:

$$\frac{\partial u}{\partial t} + \frac{1}{\rho}\frac{\partial p}{\partial x} = -\frac{4\tau_w}{\rho d} \quad (2)$$

When the Mach number is lower than 0.1, the incompressible flow hypothesis is confirmed [20]: for technical liquid flows, the isothermal speed of sound is larger than 1000 m/s, hence the aforementioned criteria is fully satisfied in fluid power applications. When equation (2) is multiplied by A (where $A=\pi d^2/4$ is the pipe cross-section area), integrated over the length L, and divided by the same length L, the following equation is obtained:

$$\frac{d\overline{G}}{dt} = \frac{A}{L}\Delta p - \pi d\overline{\tau_w} \quad (3)$$

where G is the mass flowrate and $\Delta p = p_{up} - p_{down}$ is the difference of the pressure signals measured along the pipe. Overlined symbols refer to the quantities that have been space-averaged. From further passages, that are detailed in [21], it can be obtained:

$$\bar{G}(t) = \langle G \rangle + \frac{A}{L}\int_0^t [\Delta p - \langle \Delta p \rangle]\, dt - \pi d \Delta\bar{\Gamma}_{fdf} \quad (4)$$

where the angular brackets denote a time-averaged variable and $\Delta\bar{\Gamma}_{fdf}$ is a function that considers the frequency dependent friction effect. Equation (4) gives the instantaneous mass flow rate by measuring the pressure difference Δp and the time-averaged flow rate $\langle G \rangle$, and the latter can be obtained via a Coriolis flowmeter installed in a low-pressure line of the hydraulic circuit or can be estimated by knowing the geometrical features of the hydraulic component under investigation.

3. Experimental facilities

The presented flowmeter has been applied to measure the flow ripples of an external gear pump [22], of an internal gear pump [23], and the flow entering a Common Rail injector during an injection event [24,25].

Figure 1 reports the schemes of the hydraulic circuits for the cases in which a volumetric pump is tested (cf. figure 1a) and when a Common Rail injection system is considered (cf. figure 1b). As can be seen, in the former case the flowmeter is installed in the pump delivery line, while in the latter it monitors the injector-feeding pipe.

Concerning the external gear pump analysis, tests have been performed for different values of pump speed, and a fixed orifice downstream the delivery line has been employed to generate the counterpressure. The tested pump features a displacement of 51.5 cc/rev, a speed in the 300-2500 rpm range and a maximum pressure of 230 bar. The delivery line consists of a steel pipe with an internal diameter, *d*, of 10 mm, and a total length equal to 700 mm. During the experimental campaign, the delivered flowrate has been acquired for different working conditions. The flowmeter is installed at a distance of about 150 mm from the delivery port.

Similarly, the internal gear pump delivers the flowrate to a steel pipe with a length of 710 mm and an internal diameter equal to 7.8 mm. At the end of the delivery line a variable orifice has been used to modify the load at a fixed pump speed. The tested internal gear pump features a displacement of 6.5 cc/rev, a maximum working pressure of 210 bar, and the speed can be selected in the 600-3600 rpm range. In this case, the flowmeter has been installed almost next to the pump, and the flowrate pertaining to different working conditions has been measured.

Diameters of the rigid pipes have been selected consistently with the pumps or the injector geometry. Concerning the pipes length, this has been selected to guarantee the consistency of the one-dimensional flow assumption. Pipes with an aspect ratio (pipe length over pipe diameter) greater than 40 have been employed, and the distance between the pressure sensors, *L*, has been selected significantly higher than $L_{min}=2a\Delta t$, where Δt=10 μs is the sample time of the acquired signal [22].

Referring to the Common Rail system, that is the most diffused fuel injection system for diesel engines [26–28], it is constituted by a high-pressure rotary pump that feeds the rail, at which four solenoid injectors are connected by means of high-pressure lines [29]. Over one of these pipes the flowmeter has been installed (cf. figure 1b). A Nanyue injector [30] has been tested to develop the numerical model. Experimental campaigns pertaining to Common Rail systems have been performed at the Moehwald-Bosch hydraulic test bench available at the ICE Laboratory at the Politecnico di Torino. The injected flowrate is measured by means of a HDA flowmeter, and the current signal provided to the injector pilot stage is detected by a current clamp.

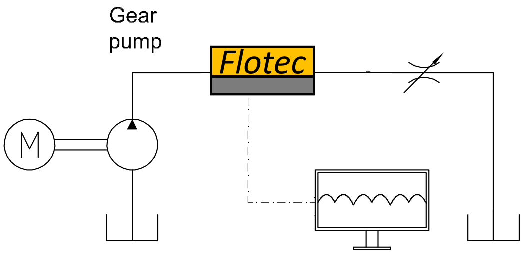

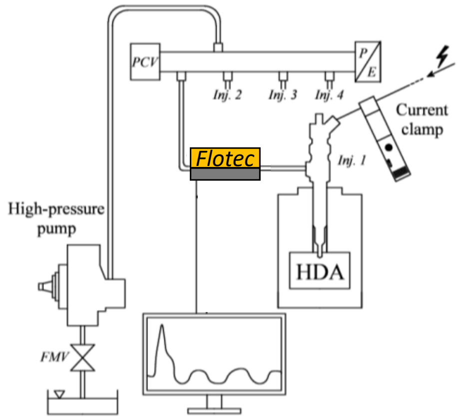

(a) (b)

Figure 1. Tested hydraulic layouts: (a) Gear pump, (b) Common Rail injection system.

4. Numerical models

The 3D numerical models pertaining to the gear pumps, together with their delivery lines, have been built with the commercial software SimericsMP+, where the governing equations are discretized by means of finite volume method. Further details about the models of the external gear pump and the internal one can be found in [22] and [23], respectively. After a grid independence analysis, simulations have been performed and the models have been validated by comparing the numerical pressure traces detected along the pump delivery lines, in correspondence of the pressure sensors locations, with the corresponding experimental time histories. Figures 2 and 3 show that the numerical pressures and the experimental ones are in very good agreement. In particular, figure 2 is referred to the external gear pump, with a velocity of 1750 rpm and a load of 133 bar, while figure 3 reports the data referring to the internal gear pump, for a speed equal to 1500 rpm and a load of 4.5 bar. Due to the good agreement between the numerical pressure traces (represented by dashed lines) and the experimental ones (plotted as continuous lines), the 3D models have been considered satisfactorily validated (validation has been performed over different working points).

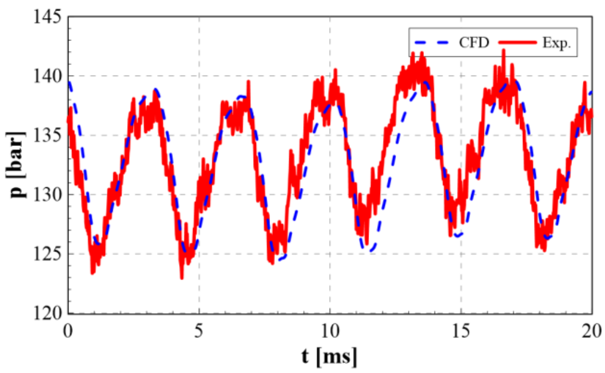

Figure 2. Validation of the 3D numerical model of the external gear pump (shaft speed: 1750 rpm, load: 133 bar).

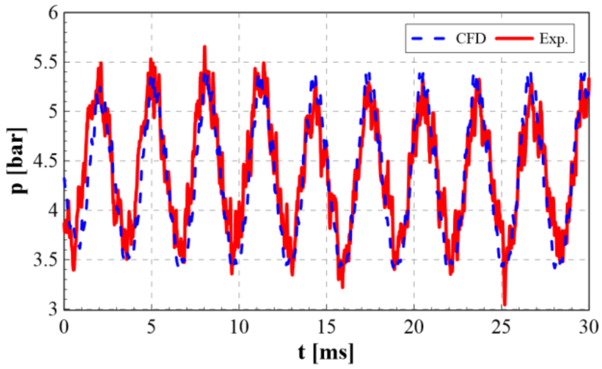

Figure 3. Validation of the 3D numerical model of the internal gear pump (shaft speed: 1500 rpm, load: 4.5 bar).

Concerning the Common Rail diesel injection system, a 1D numerical diagnostic tool has been used to assess the consistency of the presented algorithm for the flowrate determination. This numerical tool considers the main characteristic of the hydraulic circuit, the electromagnetic setup, and the mechanical components. It is constituted by a network of 0D chambers connected by 1D lines, for which a Lax-Wendroff scheme is employed to solve them.

The pressure time history measured inside the rail is applied to a 0D chamber as a boundary condition, together with the current signal to the pilot stage. The selected boundary conditions allow the possibility to avoid any inaccuracy in the high-pressure pump and in the Electronic Control Unit modeling [31]. The flow through the hydraulic circuit is assumed as isothermal. Further details of the numerical model can be found in [32]. The model validation has been performed by means of a comparison of both the pressure trace measured close to the injector along the rail-to-injector pipe (namely, p_{down}) and the injected flowrate time history (G_{inj}), measured by the HDA, with the corresponding numerical traces. This comparison is presented in figure 4, where a single injection with a nominal rail pressure of 900 bar and an energizing time of 500 μs is considered. As can be inferred, both the pressure trace and the injected flowrate numerical traces (represented by lines) are in very good agreement with the experimental ones (reported with symbols), therefore, the model can be considered validated (validation has been performed over different working points, for both single and pilot-main injections).

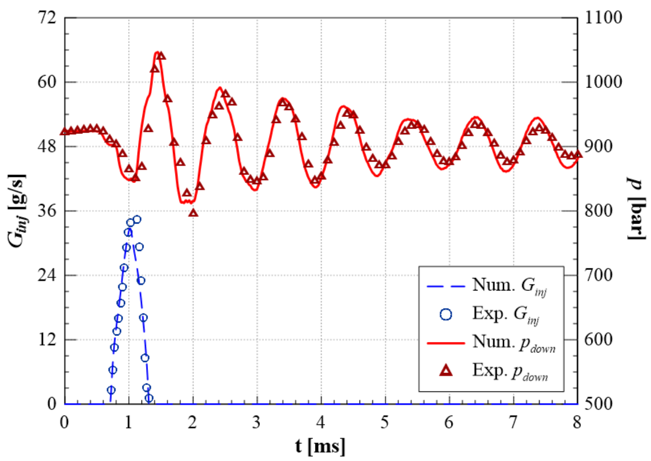

Figure 4. Validation of the 1D numerical model of the Common Rail diesel injection system (rail pressure: 900 bar, energizing time: 500 μs).

5. Validation of the flowrate measurements

The absence of a master instrument that is capable to measure a high-pressure liquid flowrate that can be employed as a reference to verify the consistency of the proposed algorithm justifies the use of the abovementioned validated numerical models.

Figure 5 shows the measured flowrate along the delivery line fed by the investigated external gear pump as a continuous line, compared with the one provided by the 3D numerical model, represented as a dashed line. The pump speed was set to 1000 rpm and the pressure load along the line was equal to 45 bar. The time-averaged flowrate in equation (4) has been determined by knowing the pump displacement and the rotational speed [22]. As can be inferred from figure 5, the numerical flowrate and the measured one result in very good agreement.

Figure 6 presents the same results of figure 5, referred to the internal gear pump. In this case, the pump speed was equal to 1500 rpm, and the load was set to 9.5 bar. For this case, the time-average flowrate has been determined by means of a Coriolis flowmeter installed downstream of the variable orifice. The comparison in figure 7 between the numerical flowrate and the measured one results to be very satisfactory.

Finally, figure 7 reports the flowrate entering the injector during an injection event obtained by the 1D numerical model (as a dashed line) and experimentally measured (as a continuous line), for a single injection featuring a rail pressure of 900 bar and an energizing time equal to 500 μs. The time-averaged flowrate required by equation (4) has been calculated by knowing the injected mass and the flowrate discharged by the pilot stage (measured by means of a Coriolis flowmeter). Even for the Common Rail injection system, the measured flowrates satisfactorily overlap the numerical one, providing a further validation of the employed measuring device. The pressure waves generated during the injection and at its end travel forth and back along the injector-feeding pipe. These waves locally induce to the negative flowrate that can be noticed in figure 7, which correspond to reverse flows from the injector to the rail (the positive direction of the 1D flow velocity in equation (1) and equation (2) is from the left to the right, hence, referring to figure 1b, from the rail to the injector).

Due to the very satisfactory results obtained by the validation of the proposed measurement algorithm, this measuring device can be employed during experimental campaigns, providing an additional measurement that can be imposed as boundary condition for numerical model or as a reference for model-validation purposes. Moreover, if a Common Rail injection system is considered, for either a diesel injector or a GDI one, this flowmeter can be used to obtain a feedback signal to set-up a closed loop control to correct inaccuracies of the injected mass [24,33].

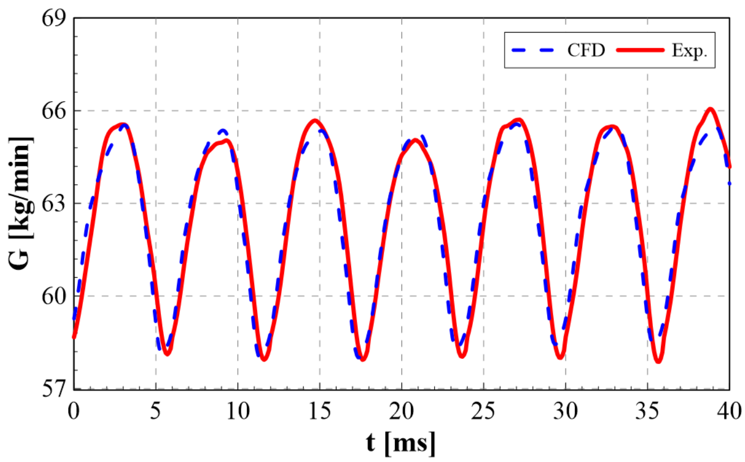

Figure 5. Comparison between the numerical flowrate delivered by the external gear pump and the experimental one (shaft speed: 1000 rpm, load: 45 bar).

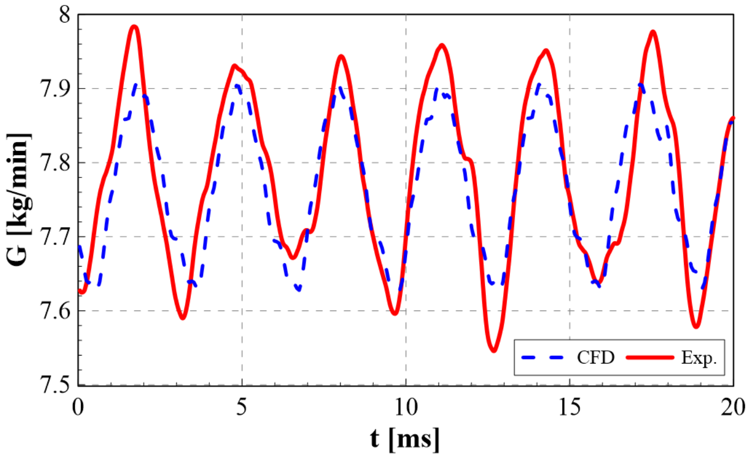

Figure 6. Comparison between the numerical flowrate delivered by the internal gear pump and the experimental one (shaft speed: 1500 rpm, load: 9.5 bar).

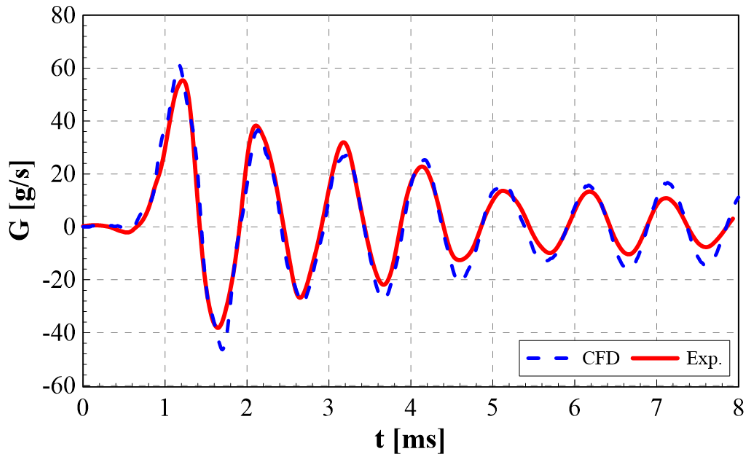

Figure 7. Comparison between the numerical flowrate entering the injector and the experimental one (rail pressure: 900 bar, energizing time: 500 μs).

6. Conclusions

A new flowmeter that is capable to measure the instantaneous high-pressure flowrate, labelled as Flotec, has been presented. The flowmeter algorithm is based on the measure of two pressure time histories, at a certain distance, along the monitored pipe. By applying the Euler equations under the incompressible flow hypothesis, an ordinary differential equation of the instantaneous flowrate can be obtained as a function of the measured pressure signals and the value of the averaged flowrate. The latter can be measured by means of a low-pressure flowmeter, such as a Coriolis flowmeter, or it can be estimated based on the geometrical features of the monitored device. Due to the absence of a master instrument that is capable to measure an instantaneous high-pressure flowrate, the presented flowmeter has been validated by means of numerical tools. In particular, 3D models of an external gear pump and of an internal gear pump have been developed to obtain the numerical flowrate along the delivery line, and a 1D diagnostic tool for a Common Rail injection system has been prepared to monitor the flowrate entering the injector during an injection event. The numerical models have been successfully validated by comparing the numerical pressure signals with the experimental traces. Therefore, the abovementioned numerical flowrates from the validated models have been compared with the ones provided by the Flotec flowmeter. The experimental flowrates and the numerical ones were in very satisfactory agreement, leading to a robust validation of the presented instantaneous high-pressure flowmeter.

References

[1] Catania A E, Ferrari A and Manno M 2008 Development and Application of a Complete Multijet Common-Rail Injection-System Mathematical Model for Hydrodynamic Analysis and Diagnostics *J Eng Gas Turbine Power* **130**
[2] De Souza I, Sarkar A, Anand A, Sarkar M, Kumar J S, Gour A S and Rao V V 2021 Calibration of a Cryogenic Turbine-Based Volumetric Flow Meter (CTVFM) Using Sub-Cooled Liquid Nitrogen and Solution for Its Practical Issues *IEEE Sens J* **21** 12077–83
[3] Gaskin I, Shapiro E and Drikakis D 2011 Theoretical, Numerical, and Experimental Study of the Time of Flight Flowmeter *J Fluids Eng* **133**
[4] Lee B, Cheesewright R and Clark C 2004 The dynamic response of small turbine flowmeters in liquid flows *Flow Measurement and Instrumentation* **15** 239–48
[5] Cheesewright R, Atkinson K N, Clark C, ter Horst G J P, Mottram R C and Viljeer J 1996 Field tests of correction procedures for turbine flowmeters in pu satile flows *Flow Measurement and Instrumentation* **7** 7–17
[6] Džemić Z, Širok B and Bizjan B 2018 Turbine flowmeter response to transitional flow regimes *Flow Measurement and Instrumentation* **59** 18–22
[7] Dong J, Jing C, Peng Y, Liu Y, Ren H and Liu X 2018 Study on the measurement accuracy of an improved cemented carbide orifice flowmeter in natural gas pipeline *Flow Measurement and Instrumentation* **59** 52–62
[8] Raheem A, Siddiqi A S B, Ibrahim A, Ullah A and Inayat M H 2021 Evaluation of multi-holed orifice flowmeters under developing flow conditions – An experimental study *Flow Measurement and Instrumentation* **79** 101894
[9] Moosa M and Hekmat M H 2019 Numerical investigation of turbulence characteristics and upstream disturbance of flow through standard and multi-hole orifice flowmeters *Flow Measurement and Instrumentation* **65** 203–18
[10] Head V P 1960 Discussion: "Small-Diameter-Orifice Metering" (Filban, T. J., and Griffin, W. A., 1960, ASME J. Basic Eng., 82, pp. 735–738) *Journal of Basic Engineering* **82** 739–739
[11] Doebelin E O and Manik D N 2007 *Measurement systems: application and design* (McGraw-Hill)
[12] Wang T and Baker R 2014 Coriolis flowmeters: a review of developments over the past 20 years, and an assessment of the state of the art and likely future directions *Flow Measurement and Instrumentation* **40** 99–123
[13] Zhao J, Grekhov L and Yue P 2020 Limit of Fuel Injection Rate in the Common Rail System under Ultra-High Pressures *International Journal of Automotive Technology* **21** 649–56
[14] Li X, Li D, Liu J, Ajmal T, Aitouche A, Mobasheri R, Rybdylova O, Pei Y and Peng Z 2022 Comparative Study on the Macroscopic Characteristics of Gasoline and Ethanol Spray from a GDI Injector under Injection Pressures of 10 and 60 MPa *ACS Omega* **7** 8864–73
[15] Gul S, Shiriyev J, Singhal V, Erge O and Temizel C 2021 Advanced materials and sensors in well logging, drilling, and completion operations *Sustainable Materials for Oil and Gas Applications* (Elsevier) pp 93–123
[16] Kulite 2007 *Innovative Piezoresistive Transducers*
[17] Ferrari A and Zhang T 2021 Benchmark between Bosch and Zeuch method–based flowmeters for the measurement of the fuel injection rate *International Journal of Engine Research* **22** 316–27
[18] Ferrari A, Jin Z, Vento O and Zhang T 2021 An injected quantity estimation technique based on time–frequency analysis *Control Eng Pract* **116**
[19] Ferrari A and Vento O 2020 Influence of Frequency-Dependent Friction Modeling on the Simulation of Transient Flows in High-Pressure Flow Pipelines *Journal of Fluids Engineering, Transactions of the ASME* **142**
[20] Batchelor G K 2000 *An Introduction to Fluid Dynamics* (Cambridge University Press)

[21] Ferrari A and Pizzo P 2016 Optimization of an Algorithm for the Measurement of Unsteady Flow-Rates in High-Pressure Pipelines and Application of a Newly Designed Flowmeter to Volumetric Pump Analysis *J Eng Gas Turbine Power* **138**
[22] Corvaglia A, Ferrari A, Rundo M and Vento O 2021 Three-dimensional model of an external gear pump with an experimental evaluation of the flow ripple *Proc Inst Mech Eng C J Mech Eng Sci* **235**
[23] Ferrari A, Fresia P, Rundo M, Vento O and Pizzo P 2022 Experimental Measurement and Numerical Validation of the Flow Ripple in Internal Gear Pumps *Energies (Basel)* **15**
[24] Ferrari A, Novara C, Paolucci E, Vento O, Violante M and Zhang T 2018 Design and rapid prototyping of a closed-loop control strategy of the injected mass for the reduction of CO2, combustion noise and pollutant emissions in diesel engines *Appl Energy* **232**
[25] Ferrari A, Novara C, Paolucci E, Vento O, Violante M and Zhang T 2018 A new closed-loop control of the injected mass for a full exploitation of digital and continuous injection-rate shaping *Energy Convers Manag* **177**
[26] d'Ambrosio S, Mancarella A and Manelli A 2022 Utilization of Hydrotreated Vegetable Oil (HVO) in a Euro 6 Dual-Loop EGR Diesel Engine: Behavior as a Drop-In Fuel and Potentialities along Calibration Parameter Sweeps *Energies (Basel)* **15** 7202
[27] Cococcetta F, Finesso R, Hardy G, Marello O and Spessa E 2019 Implementation and Assessment of a Model-Based Controller of Torque and Nitrogen Oxide Emissions in an 11 L Heavy-Duty Diesel Engine *Energies (Basel)* **12** 4704
[28] Ventura L, Finesso R and Malan S A 2023 Development of a Model-Based Coordinated Air-Fuel Controller for a 3.0 dm3 Diesel Engine and Its Assessment through Model-in-the-Loop *Energies (Basel)* **16** 907
[29] Ferrari A, Novara C, Vento O, Violante M and Zhang T 2023 A novel fuel injected mass feedback-control for single and multiple injections in direct injection systems for CI engines *Fuel* **334**
[30] Ferrari A, Jin Z, Mittica A, Vento O, Zhang T, Ouyang L and Tan S 2020 Application of the common-feeding injection system layout to light duty commercial vehicle diesel engines *ASME 2019 Internal Combustion Engine Division Fall Technical Conference, ICEF 2019*
[31] Ferrari A and Vento O 2023 Thermal effects on Common Rail injection system hydraulic performance *International Journal of Engine Research* 146808742311624
[32] Jin Z, Vento O, Zhang T, Ferrari A, Mittica A, Ouyang L and Tan S 2021 Numerical-experimental optimization of the common-feeding injection system concept for application to light-duty commercial vehicles *Journal of Energy Resources Technology, Transactions of the ASME* **143**
[33] Ferrari A, Pizzo P and Vento O 2023 Investigation of a GDI injector with an innovative flowmeter for high-pressure transient flows *International Journal of Engine Research*